Gastro Hep Advances 2024;3:761–772

ORIGINAL RESEARCH—CLINICAL

Pancreatic Juice-Derived microRNA-4516 and microRNA-4674 as Novel Biomarkers for Pancreatic Ductal Adenocarcinoma

Takahiko Sakaue,[1,2,3] Hironori Koga,[1,2] Hideki Iwamoto,[1,2] Toru Nakamura,[1,2] Atsutaka Masuda,[1,2] Toshimitsu Tanaka,[1,2,4] Hiroyuki Suzuki,[1,2] Hideya Suga,[5] Shingo Hirai,[1] Toru Hisaka,[6] Yoshiki Naito,[7] Keisuke Ohta,[8] Kei-ichiro Nakamura,[8] Karuppaiyah Selvendiran,[3] Yoshinobu Okabe,[1] Takuji Torimura,[9] and Takumi Kawaguchi[1]

[1]Division of Gastroenterology, Department of Medicine, Kurume University School of Medicine, Kurume, Japan; [2]Liver Cancer Research Division, Kurume University Research Center for Innovative Cancer Therapy, Kurume, Japan; [3]Division of Gynecologic Oncology, Department of Obstetrics/Gynecology, The Ohio State University Wexner Medical Center, Columbus, Ohio; [4]Center for Multidisciplinary Treatment of Cancer, Kurume University Hospital, Kurume, Japan; [5]Department of Gastroenterology and Hepatology, Yanagawa Hospital, Yanagawa, Japan; [6]Department of Surgery, Kurume University School of Medicine, Kurume, Japan; [7]Department of Clinical Laboratory Medicine, Kurume University Hospital, Kurume, Japan; [8]Division of Microscopic and Developmental Anatomy, Department of Anatomy, Kurume University School of Medicine, Kurume, Japan; and [9]Department of Gastroenterology, Omuta City Hospital, Omuta, Japan

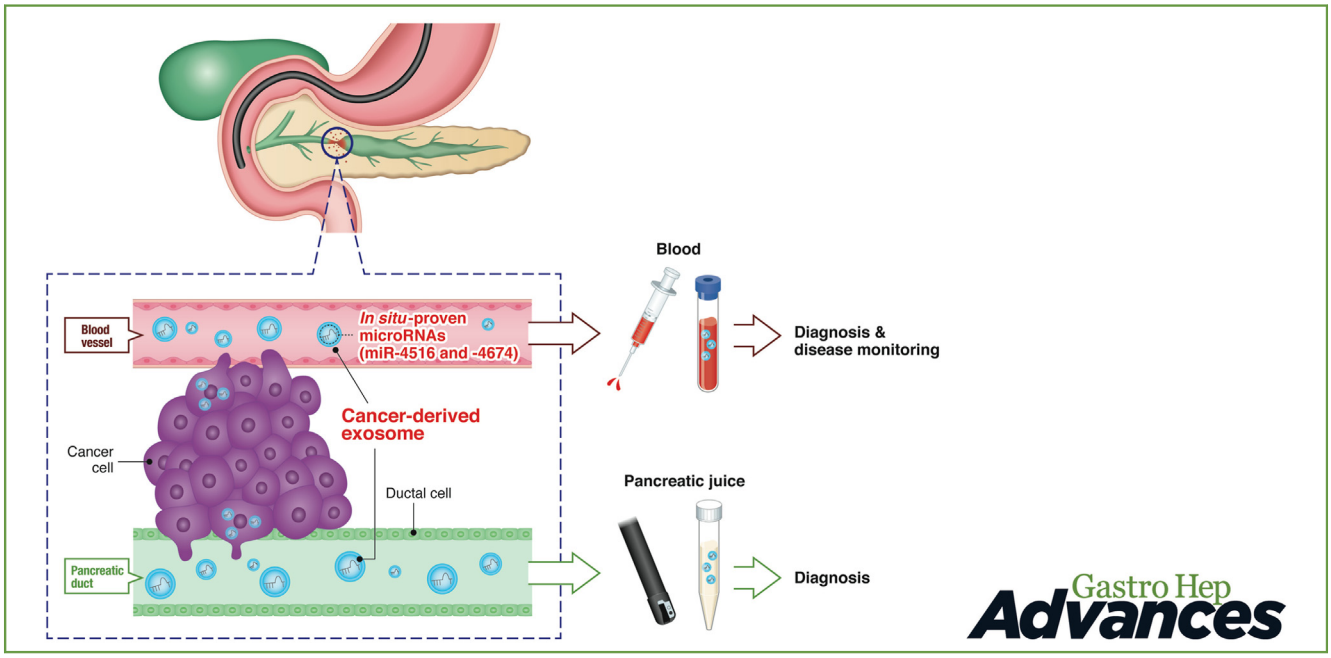

BACKGROUND AND AIMS: Precise diagnostic biomarkers are urgently required for pancreatic ductal adenocarcinoma (PDAC). Therefore, the aim of this study was to identify PDAC-specific exosomal microRNAs (Ex-miRs) from pancreatic juice (PJ) and evaluate their diagnostic potential. **METHODS:** Exosomes in PJ and serum were extracted using ultracentrifugation and confirmed morphologically and biochemically. PDAC-specific Ex-miRs were identified using our original miR arrays, in which "Ex-miRs derived from the PJ of patients with chronic pancreatitis (CP)" were subtracted from Ex-miRs commonly expressed in both "human PDAC cell lines" and "the PJ of patients with PDAC." We verified the expression of these miRs using quantitative real-time reverse transcription polymerase chain reaction. Changes in serum Ex-miR levels were assessed in 2 patients with PDAC who underwent curative

Abbreviations used in this paper: **AUC, area under the curve; CA19-9, carbohydrate antigen 19-9; CEA, carcinoembryonic antigen; CP, chronic pancreatitis; CRC, colorectal cancer; CT, computed tomography; ERCP, endoscopic retrograde cholangiopancreatography; EUS, endoscopic ultrasound; EUS-FNA, endoscopic ultrasound-guided fine-needle aspiration; Ex, exosome; HCC, hepatocellular carcinoma; HD, healthy donors; IPMN, intraductal papillary mucinous neoplasm; ISH, in situ hybridization; miR, microRNA; NTA, nanoparticle tracking analysis; PBS, phosphate-buffered saline; PDAC, pancreatic ductal adenocarcinoma; PJ, pancreatic juice; PJC, pancreatic juice cytology; qRT-PCR, quantitative real-time reverse transcription polymerase chain reaction; ROC, receiver operating characteristic; S, serum; SMA, superior mesenteric artery; TEM, transmission electron microscopy.**

Most current article

2772-5723
https://doi.org/10.1016/j.gastha.2024.04.011

resection. In situ hybridization was performed to directly visualize PDAC-specific miR expression in cancer cells. **RESULTS:** We identified novel Ex-miR-4516 and Ex-miR-4674 from the PJ of patients with PDAC, and they showed 80.0% and 81.8% sensitivity, 80.8% and 73.3% specificity, and 90.9% and 80.8% accuracy, respectively. The sensitivity, specificity, and accuracy of a triple assay of Ex-miR-4516/4674/PJ cytology increased to 93.3%, 81.8%, and 88.5%, respectively. In serum samples (n = 88), the sensitivity, specificity, and accuracy of Ex-miR-4516 were 97.5%, 34.3%, and 68%, respectively. Presurgical levels of serum-derived Ex-miR-4516 in 2 patients with relatively early disease stages declined after curative resection. In situ hybridization demonstrated that Ex-miR-4516 expression exclusively occurred in cancer cells. **CONCLUSION:** Liquid assays using the in situ-proven Ex-miR-4516 may have a high potential for detecting relatively early-stage PDAC and monitoring its clinical course.

Keywords: Exosomes; Extracellular Vesicles; Cancer Early Detection; Liquid Biopsy

Introduction

Pancreatic ductal adenocarcinoma (PDAC) is a malignant tumor with extremely poor prognosis and a 5-year survival rate of 9%,[1] which is attributed to difficulties in early disease detection.[2,3] However, the reported survival rate for stage 0 intraepithelial pancreatic cancer and tumors with a diameter $\leq$1 cm is >80%; thus, early diagnosis using precise biomarkers is essential for improving PDAC prognosis.[4]

Currently, carcinoembryonic antigen (CEA), a glycoprotein, and carbohydrate antigen 19-9 (CA19-9), a glycan antigen, are tumor markers for PDAC in clinical practice. Although CA19-9 is the most specific diagnostic marker for PDAC, its overall sensitivity is 70%–90%.[5] Further, the usefulness in early PDAC diagnosis is limited because it has a sensitivity of 4.7%–55.6%[4,6] and 50%[7] for stage I PDAC and tumors with a diameter $\leq$2 cm, respectively. Regarding the sensitivity of pancreatic juice (PJ) pancreatic juice cytology (PJC) for PDAC, the reported sensitivity before brushing is 21.3% and that after brushing is 48.8% and 65.8%.[8,9] Moreover, the obtained results are not always satisfactory and inter-institutional disparity is another major issue.

Exosomes are lipid-bilayer-enclosed extracellular vesicles with a diameter of 50–150 nm.[10,11] They contain nucleic acids and proteins, which mediate intercellular communication.[10,12,13] In the case of tumor-derived exosomes, intra-exosomal contents are believed to enrich tumor-specific genomic information.[14,15] Therefore, they can be highly useful as tumor markers. Currently, serum microRNA (miR) and circulating tumor cells are under consideration in developing promising assays for early detection of PDAC; however, further research is required to determine the practical application of these biomarkers.[16]

The aims of this study were to identify PDAC-specific exosomal microRNAs (Ex-miRs) from PJ, found in direct contact with PDAC in the pancreatic duct, and evaluate their diagnostic potential against known tumor markers and PJC.

Material and Methods

Patients and Samples

This study was designed as an observational study; it was approved by the Ethical Committee of Kurume University (Kurume, Japan) (Study registration no: 351) and Yanagawa Hospital (Yanagawa, Japan), was conducted according to the Ethical Guidelines for Human Genome/Gene Research enacted by the Japanese Government, and adhered to the recommendations specified in the Declaration of Helsinki. Interventional approaches were not applied in this study. Written informed consent for the use of PJ and serum was obtained from all patients and healthy donors (HDs) prior to specimen collection, and planned analyses regarding early diagnostic markers for pancreatic cancer were disclosed. Patient eligibility criteria were age 20 or older, written consent, histologically verified malignant tumors (PDAC, hepatocellular carcinoma (HCC), and colorectal cancer (CRC)), chronic pancreatitis (CP) and intraductal papillary mucinous neoplasm (IPMN) with no tumor development during the 12-month observation, and negative medical history for any other malignant disease. HD eligibility criteria were age 20 or older, written consent, and negative medical history for any malignant disease. After PJ and blood collection, the PJ and serum samples were first utilized for assessing PJC and blood biochemistry, respectively. The samples remaining after these tests were used for further analyses. Eighty patients who visited Kurume University Hospital (Kurume, Japan) and Yanagawa Hospital from January 2018 to January 2021 were enrolled in this study (Table A1). Fifty patients had PDAC, 12 had CP, 4 had IPMN, 8 had HCC, and 6 had CRC. Eight HD patients were also included in this study. PJ samples obtained from 15 patients with PDAC and 11 patients with CP (Table 1) through endoscopic retrograde cholangiopancreatography (ERCP) were used to assess the diagnostic values of PDAC-specific Ex-miRs. The serum analysis of miRs included 75 cases (40 PDAC and 35 non-PDAC) (Table 1). The non-PDAC group included 9 CP, 4 IPMN, 8 HCC, 6 CRC, and 8 HD cases.

PJ and Serum Samples

PJ collected at the time of ERCP or from the endoscopic nasobiliary drainage tube was used as a specimen. Serum was simultaneously obtained from patients within 2 days before and after PJ collection. Both samples were stored at −80 °C until use.

Cell Lines and Culture Conditions

The following human PDAC cell lines were used: PANC-1 (American Type Culture Collection (ATCC, Manassas, VA, USA) CRL-1469), BxPC-3 (ATCC CRL-1687), and MIA PaCa-2 (ATCC CRL-1420). All cell lines were cultured in Dulbecco's modified Eagle medium (DMEM) (Wako, Osaka, Japan) supplemented with 10% heat-inactivated (56 °C, 30 min) exosome-depleted fetal bovine serum (System Biosciences, Palo Alto, CA, USA), 100 units/mL penicillin, and 100 mg/mL streptomycin (Nacalai Tesque, Kyoto, Japan) at 37 °C in a humidified atmosphere

Table 1. Characteristics of Patients Included for PJ-Based Diagnosis and Serodiagnosis

PJ-based diagnosis	PDAC (n = 15)	CP (n = 11)	*P* value
Age, y [median (range)]	70 (55–83)	64 (41–91)	.81
Gender, male/female	9/6	9/2	.39
Location, head/body/tail	9/4/2	–	–
TS, TS1/TS2/TS3/TS4	3/8/4/0	–	–
Stage, 0/I/II/III/IV	0/0/6/3/6	–	–
T factor, 1/2/3/4	0/0/10/5	–	–
N factor, 0/1	6/9	–	–
M factor, 0/1	9/6	–	–
CEA, ng/mL [median (range)]	3.5 (1.8–33.5)	3.9 (1.8–7.7)	.26
CA19-9, U/mL [median (range)]	271 (<1.0–>12,000)	10.3 (<2.0–65.1)	.04
PJC, positive/negative/none	9/2/4	0/11/0	<.0001
Serodiagnosis	**PDAC (n = 40)**	**Non-PDAC* (n = 35)**	***P* Value**
Age, y [median (range)]	65.5 (45–83)	63 (34–91)	.22
Gender, male/female	19/21	22/13	.18
Location, head/body/tail	22/14/4	–	–
TS, TS1/TS2/TS3/TS4	8/25/6/1	–	–
Stage, 0/I/II/III/IV	0/6/8/4/22	–	–
T factor, 1/2/3/4	4/2/18/16	–	–
CEA, ng/mL [median (range)]	4.95 (0.4–1381)	4.75 (2–2977)	.17
CA19-9, U/mL [median (range)]	118 (<1.0–26,312)	23.25 (<2.0–2015)	.05

non-PDAC*: CP: n = 9, HD: n = 8, IPMN: n = 4, HCC: n = 8, CRC: n = 6.
CA19-9, carbohydrate antigen 19-9; CEA, carcinoembryonic antigen; CP, chronic pancreatitis; CRC, colorectal cancer; HCC, hepatocellular carcinoma; HD, heathy donor; IPMN, intraductal papillary mucinous neoplasm; PDAC, pancreatic ductal adenocarcinoma; PJC, pancreatic juice cytology; TS, tumor size.

containing 5% CO_2. Cells were used within 3–8 passages after recovery from frozen stocks. Cell passages were performed at the 70%–80% confluent state. Negative test results for mycoplasma contamination were ascertained in all cell lines in our study using LookOut® Mycoplasma PCR Detection Kit (Sigma-Aldrich, Saint Louis, MO, USA).

Isolation and Characterization of Exosomes

Exosomes were isolated from PJ by ultracentrifugation only for transmission electron microscopy (TEM) and nanoparticle tracking analysis (NTA).[17] Briefly, 2 mL of PJ was filtered through a 0.8 μm filter and the filtrate was added to an equal volume of 5% glutaraldehyde. The solution was mixed by inversion and then fixed for 1 h at 4 °C. The mixture was centrifuged at 300 × *g* for 10 min at 4 °C, followed by centrifugation at 2000 × *g* for 10 min at 4 °C to discard cellular debris. Then, the supernatant was centrifuged at 10,000 × *g* for 30 min at 4 °C to remove the remaining debris. Thereafter, the supernatant was ultracentrifuged at 100,000 × *g* for 90 min at 4 °C. Next, the exosome pellet was washed in 500 μL 1X phosphate-buffered saline (PBS), followed by ultracentrifugation at 100,000 × *g* for 90 min at 4 °C. The supernatant was discarded, and pelleted exosomes were solidified by adding 15 μL of 1% agar for TEM and resuspended in 50 μL of PBS for NTA. Both samples were stored at 4 °C until analysis the next day. Otherwise, exosomes were isolated from PJ and serum using the exoEasy Maxi Kit (Qiagen, Hilden, Germany) according to the manufacturer's protocol. Upon reaching 70%–80% cell confluence, exosomes were extracted from cell lysate similarly. Exosomes used for RNA extraction were resuspended in 500 μL of TRIzol Reagent (Invitrogen/Life Technologies, Carlsbad, CA, USA) and then stored at −80 °C. Exosomes used for protein extraction were resuspended in 5X RIPA buffer (Pierce, Rockford, IL, USA) containing protease inhibitor cocktail (Nacalai Tesque, Kyoto, Japan) and Halt phosphatase inhibitor cocktail (Pierce, Rockford, IL, USA) and then stored at −20 °C. To confirm the presence of exosomes in liquid samples, common protein markers for exosomes, including CD9, CD63, CD81, and HSP70, were assessed using western blotting, as previously described.[17]

Isolation of Total RNA

Total RNA (including the miRs) was isolated from 1 mL of PJ or serum using TRIzol Reagent (Invitrogen/Life Technologies, Carlsbad, CA, USA) and purified using the miRNeasy Mini Kit (QIAGEN) according to the manufacturer's instructions. RNA samples were quantified using an ND-1000 spectrophotometer (NanoDrop Technologies, Wilmington, DE, USA), and their quality was confirmed using the Agilent 4200 TapeStation (Agilent Technologies, Santa Clara, CA, USA).

Microarray Analysis of miR Expression

A total of 100 ng total RNA from each sample was labeled using a FlashTag™ Biotin HSR RNA Labeling Kit and hybridized to the Affymetrix GeneChip® miRNA 4.0 Array according to the manufacturer's instructions. All hybridized microarrays were scanned using an Affymetrix scanner. Relative hybridization

intensities and background hybridization values were calculated using Affymetrix Expression Console™. We processed the raw CEL files for gene-level analysis with median polish summarization and quantile normalization using Affymetrix® Transcriptome Analysis Console Software and obtained normalized intensity values. To identify the upregulated or downregulated genes, we calculated ratios (nonlog-scaled fold change) from the normalized intensities of each gene for comparisons between control and experiment samples. Then, we established criteria for regulated genes: upregulated genes, ratio $\geq$2.0-fold; downregulated genes, ratio $\leq$0.5.

Quantitative Real-Time Reverse Transcription Polymerase Chain Reaction (qRT-PCR)

For qRT-PCR analysis, complementary DNA was generated from total RNA using the TaqMan® MicroRNA Reverse Transcription Kit (Applied Biosystems, Foster City, CA, USA) according to the manufacturer's protocols. Real-time PCR was then performed using the TaqMan® FAST Advanced Master Mix (Applied Biosystems) with technical triplicates on a StepOnePlusTM Real-Time PCR System (Applied Biosystems). Relative quantification of gene expression was performed using the $2^{-\Delta\Delta CT}$ method[18] in StepOne Software 2.0 (Applied Biosystems). Hsa-miR-6858-5p, the miR showing the least variation in the microarray data (when examining PJ and serum), and U6 (when examining the cell culture supernatants) were used as the reference for raw data normalization. The primer sequences used are listed in Table A2.

In Situ Hybridization (ISH)

ISH was performed using an ISH Reagent Kit (GenoStaff, Tokyo, Japan) according to the manufacturer's instructions. Tissue sections were deparaffinized with G-Nox (Nippon Genetics, Co, Ltd, Tokyo, Japan) and rehydrated using an ethanol series and PBS. The sections were then fixed with 10% neutral buffered formalin for 30 min at 37 °C, washed in distilled water, placed in 0.2% HCL for 10 min at 37 °C, washed in PBS, treated with 10 μg/mL Proteinase K (Fujifilm, Tokyo, Japan) in PBS for 10 min at 37 °C, and washed in PBS. The sections were then heat-treated in PBS for 10 min at 95 °C, cooled immediately in PBS at room temperature (RT), and placed in a Coplin jar containing 1× G-Wash (GenoStaff), which was equal to 1× SSC buffer. Hybridization was performed with 250 nM of probes in G-Hybo-L (GenoStaff) for 16 h at 40 °C. The hybridization sequences used were as follows: 5'-GGGAGAAGGGUCGGGGC-3' (miR-4516), 5'-CUGGGCUCGGGACGCGCGGCU-3' (miR-4674), and 5'-GTGTAACACGTCTATACGCCCA-3' (scramble) (QIAGEN). After hybridization, the sections were washed 3 times with 50% formamide in 2× or 0.5× G-Wash for 30 min at 40 °C and 5 times in 0.1% Tween 20 in Tris-buffered saline (TBST) at RT. After treatment with 1× G-Block (GenoStaff) for 15 min at RT, the sections were incubated with anti-DIG AP conjugate (Roche, Basel, Switzerland) diluted 1:2000 with G-Block (diluted 1/50) in TBST for 1 h at RT. The sections were then washed twice in TBST and incubated in 100 mM NaCl, 50 mM $MgCl_2$, 0.1% Tween 20, and 100 mM Tris-HCl at pH 9.5. Color reactions were performed with nitroblue tetrazolium/5-bromo-4-chloro-3-indolyl-phosphate solution (Sigma-Aldrich), followed by washing in PBS. The sections were counterstained with Kernechtrot Stain Solution (Muto Pure Chemicals, Co, Ltd, Tokyo, Japan), and mounted with G-Mount (GenoStaff), followed by Malinol (Muto Pure Chemicals). Images were obtained using a NanoZoomer S210 Digital slide scanner (C13239-01, Hamamatsu Photonics, Hamamatsu, Japan) and NDP.view 2 Plus Viewing software (U12388-02, Hamamatsu Photonics).

Cell Transduction With miR-4516 Inhibitor

PANC-1 cells were transduced with copepoda green fluorescence protein control lentiviral particles (Catalog No. SC-108084) (Santa Cruz Biotechnology, Santa Cruz, CA, USA) or LentimiRa-Off-hsa-miR-4516 Virus (Catalog No. mh36516) (Applied Biological Materials, Richmond, BC, Canada) according to the manufacturer's instructions. Briefly, 1×10^4 cells were seeded and cultured overnight in a 10% serum-containing medium. After 24 h, the medium was changed to Stemline (Thermo Fisher Scientific, Waltham, MA, USA) containing the transduction agent TransDux (Catalog No. LV850A-1) (Systems Biosciences, Palo Alto, CA, USA) and either LentimiRa-Off-has-miR-4516 Virus or copepoda green fluorescence protein control lentiviral particles were added to the cells overnight according to manufacturer's protocol. After 3 days of incubation, green fluorescence protein expression was confirmed by microscopy, and puromycin treatment (1 μg/mL) (Invitrogen) was applied to establish stably transduced cells. Single-cell clones with green fluorescence protein expression were isolated under continuous puromycin treatment. miR-4516 expression was then determined using qRT-PCR.

Cell Proliferation Assay

PANC-1 cells transduced with miR-4516 inhibitor and scrambled miR (control) were plated onto 96-well plates at a density of 3×10^3 cells/well and incubated in a medium containing 10% FBS at 37 °C for 12 h. Subsequently, the cell proliferation rates were determined using Cell Count Reagent SF (Nacalai Tesque, Kyoto, Japan) according to the manufacturer's protocol.

Statistical Analyses

All statistical analyses were performed using JMP Pro 16 software (SAS Institute Inc, Cary, NC, USA). Receiver operating characteristic (ROC) curves were constructed using each miR expression value. The area under the curve (AUC) and sensitivity and specificity values were calculated to evaluate the diagnostic potential of the candidate miRs. Statistically significant differences were assessed using unpaired Student's *t*-tests. All experimental data were expressed as mean $\pm$ standard deviation, and $P < .05$ indicated statistically significant differences.

Results

Identification of Exosomes in PJ

The presence of exosomes in PJ from patients with PDAC and CP was morphologically confirmed via TEM (Figure 1A) and NTA (Figure 1B). Approximately 100 nm-sized, round-shaped, double membrane-enclosed vesicles were observed by TEM, and they were consistent with the typical exosome structure (Figure 1A). NTA showed that the mean mode size ($\pm$standard deviation) and particle concentration of PJ-derived exosomes were 109.2 $\pm$ 6.0 nm and 2.62×10^{11} particles/mL, respectively (Figure 1B). Successful purification of exosomes

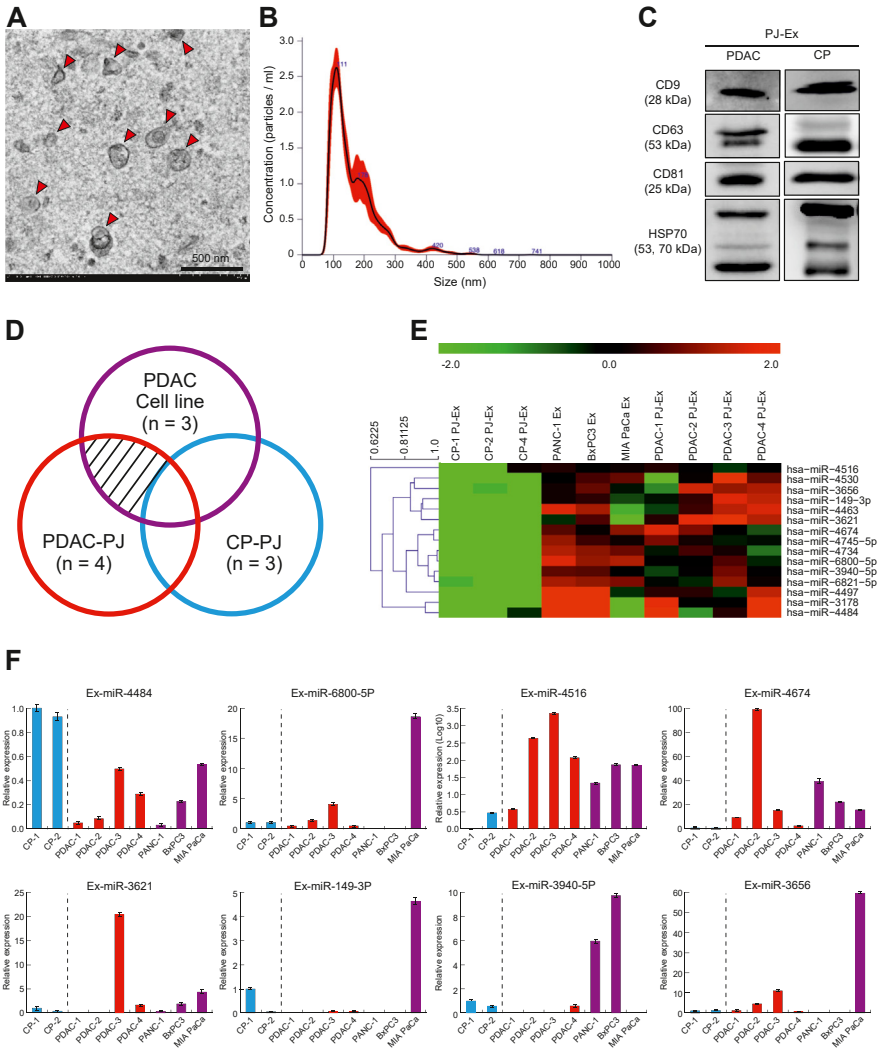

Figure 1. Characterization of PJ-derived exosomes and overview of the PDAC-specific Ex-miR identification process. (A) TEM showing the ultrastructural appearance of PJ-derived exosomes from patient CP-3. Arrowheads indicate exosomes. (B) NTA showing the size distribution of PJ-derived exosomes from patient CP-3. The black line represents the mean of 5 experiments, and the red line indicates the standard deviation. (C) Exosomes isolated from PJ were analyzed by western blotting using antibodies against exosomal markers, including CD9 (28 kDa), CD63 (53 kDa), CD81 (26 kDa), and HSP70 (53–70 kDa). A representative image of western blot analysis using samples obtained from patients PDAC-2 and CP-3 is shown. (D) Venn diagram representing a compartment of the identified PDAC-specific Ex-miRs. (E) Heat map of the miR array analysis depicts the top 15 most upregulated Ex-miRs. The samples are cell culture supernatants from 3 PDAC cell lines and PJ from 4 patients with PDAC and 3 patients with CP. (F) qRT-PCR analysis reveals the Ex-miR-4484, Ex-miR-6800-5p, Ex-miR-4516, Ex-miR-3940-5p, Ex-miR-3621, Ex-miR-149-3p, Ex-miR-4674, and Ex-miR-3656 expression in the supernatants of PDAC cell lines ($n = 3$) and PJ of PDAC ($n = 4$) and CP cases ($n = 2$). Relative values normalized to those for the control miR-6858-5P are expressed as fold-changes compared with those in patient CP-1. The results are presented as mean ± SD. CP, chronic pancreatitis; Ex, exosome; miR, microRNA; NTA, nanoparticle tracking analysis; PDAC, pancreatic ductal adenocarcinoma; PJ, pancreatic juice; TEM, transmission electron microscopy.

was confirmed by western blotting of exosome-specific proteins, such as CD9, CD63, CD81, and HSP70 (Figure 1C).

Identification of Novel PDAC-Specific Ex-miR-4516 and Ex-miR-4674 From PJ

Figure 1D shows the Venn diagram illustrating our original method. We identified the top 15 most upregulated Ex-miRs in PDAC (Figure 1E and Table A2). To validate the reproducibility of these miRs, we performed qRT-PCR and confirmed the expression of 8 out of 15 miRs (Figure 1F). Subsequently, we identified novel Ex-miR-4516 and Ex-miR-4674 as candidates for PDAC-specific Ex-miRs.

Diagnostic Potential of Ex-miR-4516 and Ex-miR-4674 in PJ

To evaluate the diagnostic value of PJ-derived Ex-miR-4516 (PJ-Ex-miR-4516) and Ex-miR-4674 (PJ-Ex-miR-

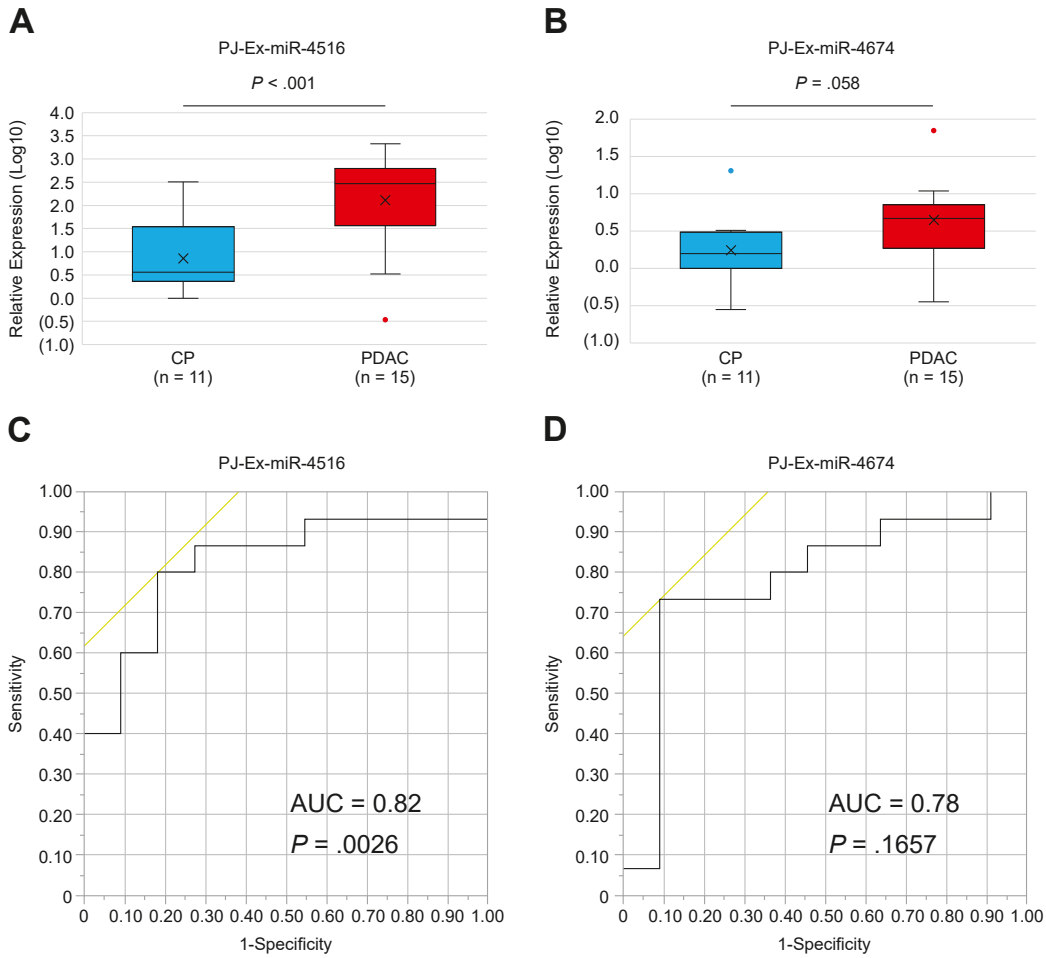

Figure 2. Diagnostic potential of PJ-Ex-miRs-4516 and -4674 for PDAC. PJ-Ex-miR-4516 (A) and -4674 (B) expression in patients with PDAC (n = 15) and CP (n = 11). Fold changes in the expression of the 2 PJ-Ex-miRs are compared with those in the patient CP-1. ROC curves for the sensitivity and specificity of PJ-Ex-miR-4516 (C) and -4674 (D), coupled with their AUC and *P* values are shown. The results are presented as mean ± SD. AUC, area under the curve; CP, chronic pancreatitis; Ex, exosome; miR, microRNA; PDAC, pancreatic ductal adenocarcinoma; PJ, pancreatic juice; ROC, receiver operating characteristic.

4674), the miR expression levels were evaluated using qRT-PCR in 26 samples (15 and 11 samples of PJ from patients with PDAC and CP, respectively). As shown in Figure 2A, PJ-Ex-miR-4516 expression was significantly higher in the PDAC group than in the CP group ($P < .001$). PJ-Ex-miR-4674 showed a trend similar to that of PJ-Ex-miR-4516, but the observed difference was not significant ($P = .058$) (Figure 2B). ROCs were generated, and the sensitivity, specificity, and accuracy were determined. The AUCs for PJ-Ex-miR-4516 and PJ-Ex-miR-4674 were 0.82 ($P = .0026$) and 0.78 ($P = .1657$) (Figure 2C and D), respectively. PJ-Ex-miR-4516 and PJ-Ex-miR-4674 showed 80% and 81.8% sensitivity, 80.8% and 73.3% specificity, and 90.9% and 80.8% accuracy, respectively. The sensitivity, specificity, and accuracy percentages of the combination of PJ-Ex-miR-4516/4674/PJC increased to 93.3%, 81.8%, and 88.5%, respectively (Table 2).

Diagnostic Potential of Ex-miR-4516 in Serum

To determine the potential of PJ-derived PDAC-specific miRs for PDAC serodiagnosis, qRT-PCR was preliminarily performed using serum samples from 4 to 5 patients with PDAC and CP, respectively, whose PJ and serum were simultaneously collected. In 2 of 4 patients with PDAC, high levels of Ex-miR-4516, but not Ex-miR-4674, were detected in both the PJ and serum samples, whereas in the patients with CP, Ex-miR-4516 was not found (Figure 3A and B). Ex-miR-4516 expression before and after radical resection in 2 patients with PDAC was determined to identify high expression levels of Ex-miR-4516 in both PJ and serum. The clinical backgrounds of the 2 cases are presented in Table A3 and Figure A1A–F. In these 2 cases, the PJ-Ex-miR-4516 and serum-derived Ex-miR-4516 (S-Ex-miR-4516) expressional levels before surgical resection were elevated, although PJC showed no obvious malignancy. Notably, S-Ex-

Table 2. Diagnostic Value of PJ-Ex-miR-4516, PJ-Ex-miR-4674, Pancreatic Juice Cytology, and S-Ex-miR-4516 in Pancreatic Ductal Adenocarcinoma

Variables	TP	FN	FP	TN	Sensitivity (%)	Specificity (%)	Accuracy (%)	PPV (%)	NPV (%)
PJ-Ex-miR-4516	12	3	2	9	80	81.8	80.8	85.7	75
PJ-Ex-miR-4674	11	4	1	10	73.3	90.9	80.8	91.7	71.4
PJ-Ex-miR-4516/4674	13	2	2	9	86.7	81.8	84.6	86.7	81.8
PJC	8	3	0	11	72.7	100	86.4	100	78.6
PJ-Ex-miR-4516/PJC	13	2	2	9	86.7	81.8	84.6	86.7	81.8
PJ-Ex-miR-4674/PJC	14	1	1	10	93.3	90.9	92.3	93.3	90.9
PJ-Ex-miR-4516/4674/PJC	14	1	2	9	93.3	81.8	88.5	87.5	90
S-Ex-miR-4516	39	1	23	12	97.5	34.3	68	62.9	92.3

Ex, exosome; FN, false negative; FP, false positive; NPV, negative predictive value; PJ, pancreatic juice; PJC, pancreatic juice cytology; PPV, positive predictive value; S, serum; TN, true negative; TP, true positive.

miR-4516 was markedly decreased at 22 months postresection in Case 1 ($P < .001$) (Figure 3C) and the serum value declined at 4 months postresection in Case 2 ($P < .001$) (Figure 3D). As the presurgical levels of S-Ex-miR-4516 in patients at a relatively early disease stage decreased after curative resection, a serum assay for Ex-miR-4516 may be used for disease detection and treatment effect monitoring.

To confirm the diagnostic ability of S-Ex-miR-4516, qRT-PCR was performed using sera from patients with PDAC, CP, IPMN, HCC, CRC, and HD. All non-PDAC patients were defined as the non-PDAC group. As shown in Figure 3E, the expression level of S-Ex-miR-4516 was significantly higher in the PDAC group than in the non-PDAC group ($P < .0001$). Next, the ROC curve was generated, and the sensitivity, specificity, and accuracy were determined. S-Ex-miR-4516 had an AUC of 0.67 ($P < .0001$) (Figure 3F) and sensitivity, specificity, and accuracy of 97.5%, 34.3%, and 68%, respectively (Table 2). The positive rate of S-Ex-miR-4516 by stage was as follows: Stage 0/I 100% (6/6); Stage II 100% (8/8); Stage III 100% (4/4), and Stage IV 95.5% (21/22) (Table A4). S-Ex-miR-4516 expression was significantly higher in the patients with PDAC than in those with CP ($P = .01$) and patients with IPMN ($P < .001$), suggesting that the miR has potential usefulness in the differential diagnosis of PDAC from other inflammatory diseases and benign neoplasms of the pancreas (Figure 3G). S-Ex-miR-4516 had an AUC of 0.66 ($P < .0001$) (Figure 3H) and sensitivity, specificity, and accuracy of 30%, 100%, and 47.2%, respectively.

Distribution of miR-4516 and miR-4674 in Resected PDAC Tissue

The high miR-4516 and miR-4674 expression in PJ-derived exosomes from patients with PDAC prompted us to perform an ISH analysis in the resected tumor specimen of the patient PDAC-4. The results revealed high expression of miR-4516 exclusively in cancer cells (Figure 4A) and much weaker expression of miR-4674 (Figure 4B). These findings strongly suggest that both miRs were produced and secreted from PDAC cells in vivo and that miR-4516 was abundant enough to be secreted into the blood flow in patients with PDAC. Indeed, in Case 1 (PDAC-4), Ex-miR-4516 was highly expressed in both PJ and serum, whereas Ex-miR-4674 was faintly expressed in both samples.

Functional Analysis of miR-4516 in PDAC Cells

In PANC-1 cells, miR-4516 was functionally suppressed using its inhibitor (Figure 5A). The inhibitor-treated cells showed a significantly decreased proliferative ability than that of the untreated cells (Figure 5B). A comprehensive gene analysis was then performed between the 2 cell groups to explore the genes targeted by miR-4516. The genes regulating cancer progression and metastasis, including *EGR1*, *DHRS3*, and *SOX21*, were found to be the targets of miR-4516 (Table A5).

Discussion

We successfully identified 2 PDAC-specific miRs in the exosomes of PJ from patients with PDAC. These 2 miRs were determined using ISH to be expressed specifically in cancer cells and were also detected in serum-derived exosomes obtained from patients. Notably, the levels of Ex-miR-4516 in serum exosomes were decreased after curative resection of relatively early-stage (stage II) PDAC, suggesting its potential for disease diagnosis as well as therapeutic efficacy monitoring.

In PDAC, although *GLYPICAN-1*[10] and *KRAS* mutations[19] in serum exosomes as well as several miRs, including known PJ-derived Ex-miRs,[20] have shown diagnostic value, their usefulness in clinical practice is yet to be confirmed. The difficulty in identifying PDAC-specific biomarkers for clinical use prompted us to use exosome-containing PJ derived from PDAC tissues. Another unique aspect of this study was the use of exosome-containing supernatants from human PDAC cell lines. These supernatants facilitated the exclusion of contamination by unwanted exosomes secreted from stromal cells in and around the PDAC tissues. Eventually, novel PDAC-specific Ex-miRs were identified in our original sets of samples coupled with miR array analysis, in which "Ex-miRs derived from the PJ of 3 patients with CP" were subtracted

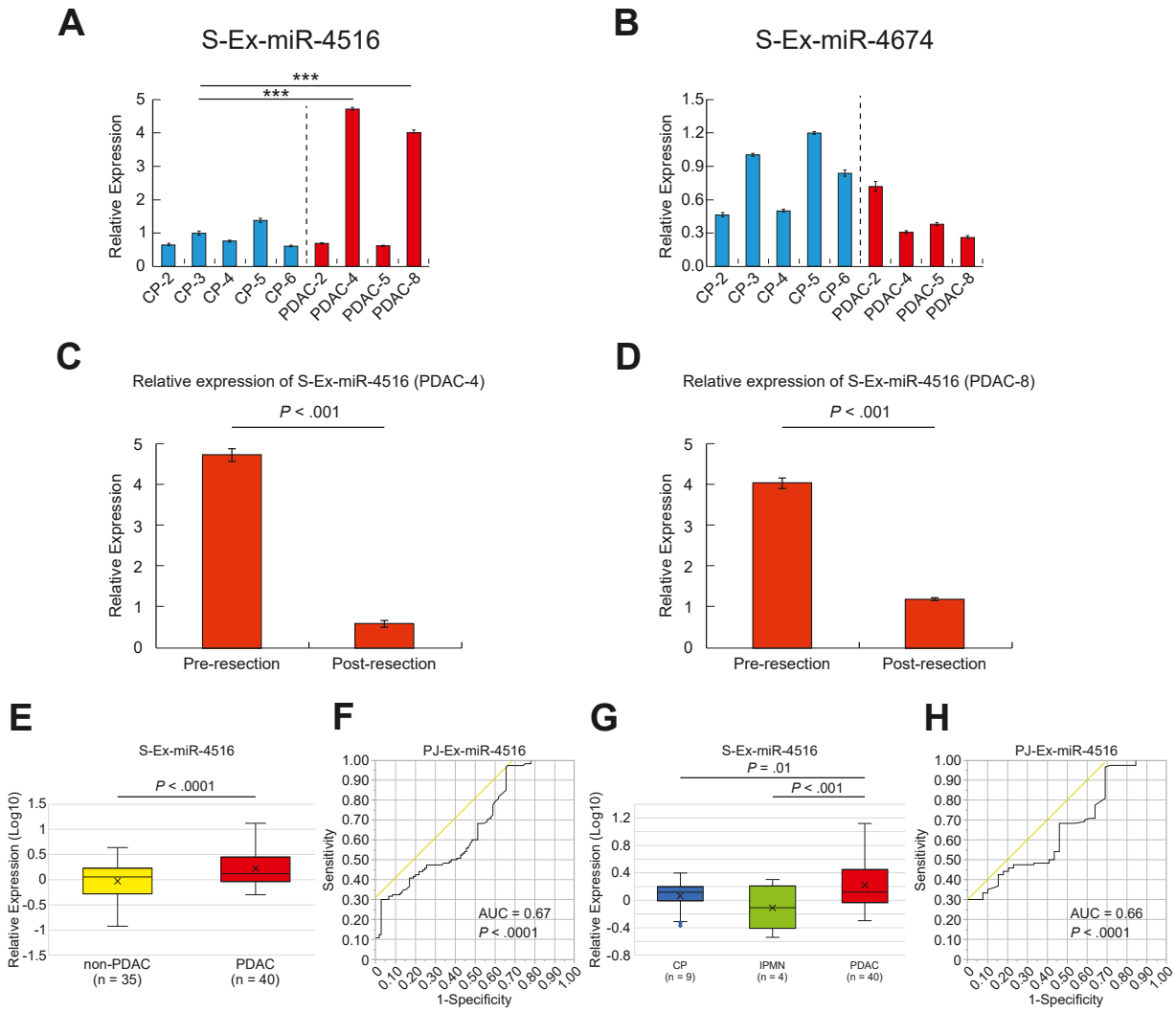

Figure 3. Detection of S-Ex-miRs-4516 and -4674 in the sera of patients with PDAC and diagnostic potential of S-Ex-miR-4516 for PDAC. (A and B) S-Ex-miR-4516 (A) and -4674 (B) expression in patients with PDAC (n = 4) and CP (n = 5), respectively. Relative fold changes compared with the expression in patient CP-3 are shown. (C and D) Expression levels of S-Ex-miR-4516 at the time of preresection and postresection in patients PDAC-4 and PDAC-8. (E) Expression levels of S-Ex-miR-4516 in the PDAC (n = 40) and non-PDAC groups (n = 35; healthy donors = 8, chronic pancreatitis = 9, intraductal papillary mucinous neoplasm = 4, hepatocellular carcinoma = 8, and colorectal cancer = 6). Relative fold-change compared with the expression level in patient CP-3 is shown. (F) ROC curve for the sensitivity and specificity of S-Ex-miR-4516 and its AUC and *P* values are presented. (G) The focus is on the differential diagnosis of PDAC from other pancreatic diseases, including CP and intraductal papillary mucinous neoplasm (IPMN). S-Ex-miR-4516 expression in patients with PDAC (n = 40) is significantly higher than that in CP (n = 9) and IPMN (n = 4). Relative fold-change compared with the expression level in patient CP-3 is shown. (H) ROC curve for pancreatic diseases is shown. The values are presented as mean ± SD. CP, chronic pancreatitis; Ex, exosome; miR, microRNA; PDAC, pancreatic ductal adenocarcinoma; S, serum.

from the miRs commonly expressed in both "Ex-miRs secreted from 3 human PDAC cell lines" and "Ex-miRs derived from the PJ of patients with 4 PDAC." This subtraction may exclude miRs, which are elevated in both PDAC and CP and are important for PDAC. However, high specificity was obtained by seeking commonalities with miRs secreted from cultured pancreatic cancer cells. Therefore, we believe that the method employed is among the best to achieve a balance between sensitivity and specificity.

ISH for Ex-miR-4516 and Ex-miR-4674 directly demonstrated that the 2 miRs were produced exclusively by PDAC cells. Further, the higher expression of Ex-miR-4516 than that of Ex-miR-4674 clearly explained why Ex-miR-4516 could be quantified in the serum exosomes of patients with PDAC. A drastic decrease in the levels of Ex-miR-4516 after curative surgery for PDAC was also indicated by the ISH findings. As ISH for miRs of interest in PDAC tissues is a strong technique to directly prove miR production,[21] it

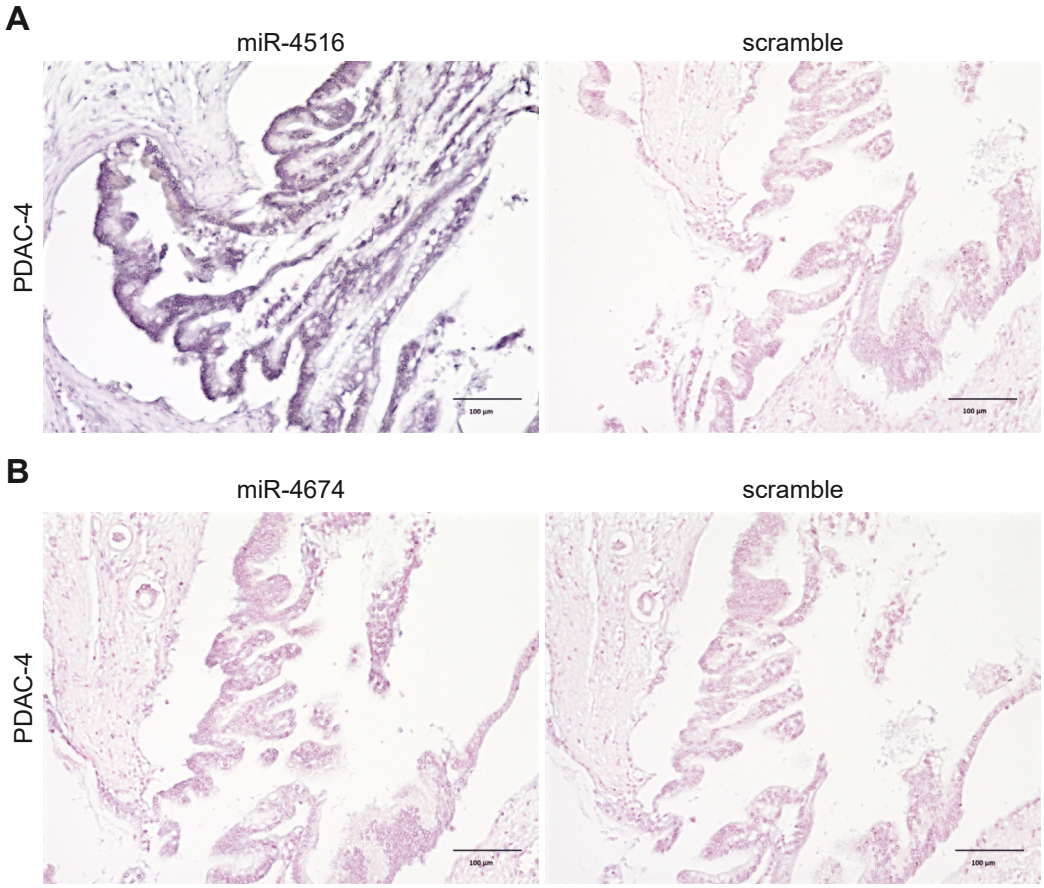

Figure 4. In situ hybridization (ISH) of miR-4516 (A) and miR-4674 (B) in PDAC tissues Representative ISH images in patient PDAC-4 using the LNA-miR-4516 probe, LNA-miR-4674 probe, and scrambled-miR control probe are shown. Scale bars, 100 μm. LNA, locked nucleic acids; miR, microRNA; PDAC, pancreatic ductal adenocarcinoma.

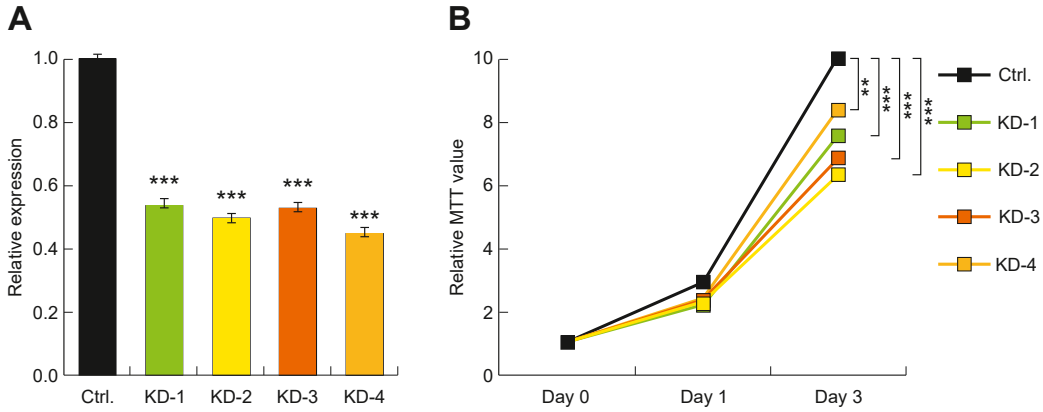

Figure 5. Functional analysis of miR-4516 in PDAC cells. (A) Expression of miR-4516 in PANC-1 cells and its knocked-down counterparts is demonstrated. Fold-change in expression is shown for miR-4516 relative to its levels in PANC-1 cells. Relative fold changes compared with the expression in PANC-1 cells are shown. The values are presented as mean ± SD. (B) MTT proliferation assay shows a significant inhibitory effect of miR-4516 knockdown on cellular proliferation in PANC-1 cells. $^{**}P < .01$, $^{***}P < .001$. miR, microRNA; PDAC, pancreatic ductal adenocarcinoma.

should be performed more frequently when validating the potential of serum biomarkers, including Ex-miRs.

The discovery of 2 specific Ex-miRs for PDAC cells encouraged us to compare their diagnostic potential using biopsy and PJC. Currently, pathological diagnosis using EUS-guided fine-needle aspiration (EUS-FNA) and PJC under ERCP is considered necessary for PDAC diagnosis.[22] If a mass-like lesion is found upon imaging, EUS-FNA is useful.

However, in minute cancer-suspected cases showing only dilatation of the main pancreatic duct, ERCP is recommended, followed by optional PJC.[22] EUS-FNA has the highest sensitivity and specificity, with an integrated sensitivity of 85%–89% and an integrated specificity of 95.8%–98% in meta-analyses.[23–26] However, it may cause needle-tract seeding of tumor cells, leading to tumor recurrence after curative resection.[27] However, ERCP shows a low sensitivity of 21.3% in ordinary PJC and 48.8% and 65.8% in cytology when the brush is rubbed back and forth.[8,9] The variations in cytological diagnosis are largely dependent on the skills and methods of endoscopists and examiners when they collect and process PJ samples.[28] Therefore, we considered that additional application of Ex-miR-4516 and Ex-miR-4674 to PJC might increase the diagnostic accuracy for PDAC. Indeed, in our retrospective analysis, the combination of measuring Ex-miRs from only 1 mL of PJ along with brushing PJ cytology demonstrated high sensitivity (>90%), specificity (∼90%), and accuracy (∼90%). Although the actual diagnostic merit should be assessed in larger prospective cohorts, the future availability of the combination assay may be proposed at least in cases that are unsuitable for EUS-FNA. In this study, false-negative results were observed in 2 cases, including a case of PDAC-5 with pancreatic mucinous carcinoma. The false negativity could be attributed to the low amount of exosome-derived RNA due to the small amount of PDAC cells and the heterogeneous distribution of exosomes in mucus-rich PJ may decrease the PCR efficiency. Two patients with CP and without PDAC showed elevated Ex-miR-4516 levels in this study. We, thus, considered the possibility of occult PDAC, and therefore suggest that they be followed up strictly.

Regarding the serological diagnosis of PDAC, the potential of Ex-miR-4516 was promising in this study. Its strong expression and high specificity in PDAC cells may provide a basis for its diagnostic capacity. Serum CA19-9 is frequently used in the current clinical practice; however, this marker is affected by sialyl-Lewis A negativity and obstructive jaundice. Therefore, serum Ex-miR-4516 can widen the target patients and contribute to health checkups and physical examinations as an alternative biomarker in the future. As various issues need to be solved before its application to disease screening, we are currently conducting a prospective study using a larger number of patients with PDAC.

Among the identified miRs, it is currently difficult to use miR-4674 for serodiagnosis. Therefore, functional analysis of miR-4516 was attempted. As for the functions of miR-4516 in cancer, previous reports have demonstrated its involvement in cancer cell proliferation, invasion, and anti-apoptosis, contributing to the infiltrative growth of tumors.[29–32] Conversely, its roles as a tumor suppressor have also been reported, and it has been shown to decrease cell proliferation, inhibit cell migration and invasion, and promote cell apoptosis.[33,34] However, its expression and function in PDAC remain largely unknown. Our gene-silencing experiment in PANC-1 cells (Figure 5A and B) suggests that miR-4516 is involved in cancer progression and metastasis[35–47] (Table A5). Interestingly, *EGR1* was identified as one of the target genes of miR-4516, whose putative role reportedly enhances the perineural invasion of PDAC cells.[37]

There are a few limitations in this study. First, a few patients with PDAC, including those with early PDAC, were enrolled in this study. Further, considering the potential tumor-promoting role of miR-4516 in other cancers, including glioblastoma[29] and breast cancer,[33] future validation studies with larger sample sizes are needed. The second limitation is that no testing was performed for the diagnostic utility of Ex-miR-4516 and Ex-miR-4674 in sialyl-Lewis A negative cases that are negative for CA19-9. Third, we included only those miR biomarkers that were significantly up-regulated in patients with PDAC compared to controls. However, it is important to recognize that this approach may lead to the missing of down-regulated candidates that may have other potential biological or clinical implications. Fourth, the functional analysis of PDAC-specific Ex-miRs was not fully completed. Therefore, its actual target genes and cells remain to be uncovered. Based on the Kaplan-Meier curves generated using The Cancer Genome Atlas database, both miR-4516 and miR-4674 appear to be promising biomarkers for poor prognosis (Figure A2A and B). Future studies on metastasis, apoptosis, and necrosis by miR inhibition will be conducted.

In conclusion, the 2 newly identified miRs specific to PDAC may increase tumor diagnostic accuracy when combined with PJC. Ex-miR-4516, which is highly expressed in cancer cells in PDAC tissues, has the potential for use in liquid assays using PJ as well as serum from patients with PDAC (published patent application number PCT/JP2021/026,597). As the target genes of Ex-miR-4516 may critically regulate PDAC cell behavior, including proliferation, further translational research is necessary to establish a novel therapeutic approach for tumor elimination.

Supplementary Materials

Material associated with this article can be found, in the online version, at https://doi.org/10.1016/j.gastha.2024.04.011.

References

1. Siegel RL, Miller KD, Fuchs HE, et al. Cancer statistics, 2021. CA Cancer J Clin 2021;71(1):7–33.
2. Warshaw AL, Fernández-del Castillo C. Pancreatic carcinoma. N Engl J Med 1992;326:455–465.
3. Rosewicz S, Wiedenmann B. Pancreatic carcinoma. Lancet 1997;349:485–489.
4. Kanno A, Masamune A, Hanada K, et al. Multicenter study of early pancreatic cancer in Japan. Pancreatology 2018;18:61–67.

5. Sharma C, Eltawil KM, Renfrew PD, et al. Advances in diagnosis, treatment and palliation of pancreatic carcinoma: 1990-2010. World J Gastroenterol 2011;17:867–897.
6. Liu J, Gao J, Du Y, et al. Combination of plasma microRNAs with serum CA19-9 for early detection of pancreatic cancer. Int J Cancer 2012;131:683–691.
7. Riker A, Libutti SK, Bartlett DL. Advances in the early detection, diagnosis, and staging of pancreatic cancer. Surg Oncol 1997;6:157–169.
8. Uchida N, Kamada H, Tsutsui K, et al. Utility of pancreatic duct brushing for diagnosis of pancreatic carcinoma. J Gastroenterol 2007;42:657–662.
9. Yamaguchi T, Shirai Y, Nakamura N, et al. Usefulness of brush cytology combined with pancreatic juice cytology in the diagnosis of pancreatic cancer: significance of pancreatic juice cytology after brushing. Pancreas 2012; 41:1225–1229.
10. Melo SA, Luecke LB, Kahlert C, et al. Glypican-1 identifies cancer exosomes and detects early pancreatic cancer. Nature 2015;523:177–182.
11. Pan BT, Teng K, Wu C, et al. Electron microscopic evidence for externalization of the transferrin receptor in vesicular form in sheep reticulocytes. J Cell Biol 1985; 101:942–948.
12. Skog J, Würdinger T, Rijn SV, et al. Glioblastoma microvesicles transport RNA and proteins that promote tumour growth and provide diagnostic biomarkers. Nat Cell Biol 2008;10:1470–1476.
13. Valadi H, Ekström K, Bossios A, et al. Exosome-mediated transfer of mRNAs and microRNAs is a novel mechanism of genetic exchange between cells. Nat Cell Biol 2007;9:654–659.
14. San Lucas FA, Allenson K, Bernard V, et al. Minimally invasive genomic and transcriptomic profiling of visceral cancers by next-generation sequencing of circulating exosomes. Ann Oncol 2016;27:635–641.
15. Lu L, Risch HA. Exosomes: potential for early detection in pancreatic cancer. Future Oncol 2016;12:1081–1090.
16. O'Neill RS, Stoita A. Biomarkers in the diagnosis of pancreatic cancer: are we closer to finding the golden ticket? World J Gastroenterol 2021;27:4045–4087.
17. Sakaue T, Koga H, Iwamoto H, et al. Glycosylation of ascites-derived exosomal CD133: a potential prognostic biomarker in patients with advanced pancreatic cancer. Med Mol Morphol 2019;52:198–208.
18. Livak KJ, Schmittgen TD. Analysis of relative gene expression data using real-time quantitative PCR and the 2(-Delta Delta C(T)) method. Methods 2001;25:402–408.
19. Allenson K, Castillo J, San Lucas FA, et al. High prevalence of mutant KRAS in circulating exosome-derived DNA from early-stage pancreatic cancer patients. Ann Oncol 2017;28:741–747.
20. Nakamura S, Sadakari Y, Ohtsuka T, et al. Pancreatic juice exosomal microRNAs as biomarkers for detection of pancreatic ductal adenocarcinoma. Ann Surg Oncol 2019;26:2104–2111.
21. Shao H, Zhang Y, Yan J, et al. Upregulated microRNA-483-3p is an early event in pancreatic ductal adenocarcinoma (PDAC) and as a powerful liquid biopsy biomarker in PDAC. Onco Targets Ther 2021; 14:2163–2175.
22. Hanada K, Okazaki A, Hirano N, et al. Diagnostic strategies for early pancreatic cancer. J Gastroenterol 2015; 50(2):147–154.
23. Banafea O, Mghanga FP, Zhao J, et al. Endoscopic ultrasonography with fine-needle aspiration for histological diagnosis of solid pancreatic masses: a meta-analysis of diagnostic accuracy studies. BMC Gastroenterol 2016; 16:108.
24. Hewitt MJ, McPhail MJW, Possamai L, et al. EUS-guided FNA for diagnosis of solid pancreatic neoplasms: a meta-analysis. Gastrointest Endosc 2012;75:319–331.
25. Puli SR, Bechtold ML, Buxbaum JL, et al. How good is endoscopic ultrasound-guided fine-needle aspiration in diagnosing the correct etiology for a solid pancreatic mass?: a meta-analysis and systematic review. Pancreas 2013;42:20–26.
26. Chen G, Liu S, Zhao Y, et al. Diagnostic accuracy of endoscopic ultrasound-guided fine-needle aspiration for pancreatic cancer: a meta-analysis. Pancreatology 2013; 13:298–304.
27. Yane K, Kuwatani M, Yoshida M, et al. Non-negligible rate of needle tract seeding after endoscopic ultrasound-guided fine-needle aspiration for patients undergoing distal pancreatectomy for pancreatic cancer. Dig Endosc 2020;32:801–811.
28. Naito Y, Tsuneki M, Fukushima N, et al. A deep learning model to detect pancreatic ductal adenocarcinoma on endoscopic ultrasound-guided fine-needle biopsy. Sci Rep 2021;11:8454.
29. Cui T, Bell EH, McElroy J, et al. miR-4516 predicts poor prognosis and functions as a novel oncogene via targeting PTPN14 in human glioblastoma. Oncogene 2019; 38:2923–2936.
30. Lai Z, Yang Y, Wang C, et al. Circular RNA 0047905 acts as a sponge for microRNA4516 and microRNA1227-5p, initiating gastric cancer progression. Cell Cycle 2019; 18:1560–1572.
31. Hao B, Shi A, Li X, et al. miR-4516 inhibits the apoptosis of RB tumor cells by targeting the PTEN/AKT signaling pathway. Exp Eye Res 2020;200:108224.
32. Borrelli N, Denaro M, Ugolini C, et al. miRNA expression profiling of 'noninvasive follicular thyroid neoplasms with papillary-like nuclear features compared with adenomas and infiltrative follicular variants of papillary thyroid carcinomas. Mod Pathol 2017;30:39–51.
33. Kim JE, Kim BG, Jang Y, et al. The stromal loss of miR-4516 promotes the FOSL1-dependent proliferation and malignancy of triple negative breast cancer. Cancer Lett 2020;469:256–265.
34. Chen S, Xu M, Zhao J, et al. MicroRNA-4516 suppresses pancreatic cancer development via negatively regulating orthodenticle homeobox 1. Int J Biol Sci 2020; 16:2159–2169.
35. Li L, Ameri AH, Wang S, et al. EGR1 regulates angiogenic and osteoclastogenic factors in prostate cancer and promotes metastasis. Oncogene 2019;38:6241–6255.
36. Liu HT, Liu S, Liu L, et al. EGR1-mediated transcription of lncRNA-HNF1A-AS1 promotes cell-cycle progression in gastric cancer. Cancer Res 2018;78:5877–5890.
37. Zhang JF, Tao LY, Yang MW, et al. CD74 promotes perineural invasion of cancer cells and mediates

neuroplasticity via the AKT/EGR-1/GDNF axis in pancreatic ductal adenocarcinoma. Cancer Lett 2021; 508:47–58.
38. Lu J, Zhong C, Luo J, et al. HnRNP-L-regulated circCSPP1/miR-520h/EGR1 axis modulates autophagy and promotes progression in prostate cancer. Mol Ther Nucleic Acids 2021;26:927–944.
39. Almairac F, Turchi L, Sakakini N, et al. ERK-mediated loss of miR-199a-3p and induction of EGR1 act as a "toggle switch" of GBM cell dedifferentiation into NANOG- and OCT4-positive cells. Cancer Res 2020; 80:3236–3250.
40. Zhang CZ, Chen SL, Wang CH, et al. CBX8 exhibits oncogenic activity via AKT/β-catenin activation in hepatocellular carcinoma. Cancer Res 2018;78:51–63.
41. Wu C, Gong S, Osterhoff G, et al. A novel four-gene prognostic signature for prediction of survival in patients with soft tissue sarcoma. Cancers 2021;13:5837.
42. Oler G, Camacho CP, Hojaij FC, et al. Gene expression profiling of papillary thyroid carcinoma identifies transcripts correlated with BRAF mutational status and lymph node metastasis. Clin Cancer Res 2008;14:4735–4742.
43. Xu Y, Wu H, Wu L, et al. Silencing of long non-coding RNA SOX21-AS1 inhibits lung adenocarcinoma invasion and migration by impairing TSPAN8 via transcription factor GATA6. Int J Biol Macromol 2020;164:1294–1303.
44. Wei C, Wang H, Xu F, et al. LncRNA SOX21-AS1 is associated with progression of hepatocellular carcinoma and predicts prognosis through epigenetically silencing p21. Biomed Pharmacother 2018;104:137–144.
45. Wei AW, Li LF. Long non-coding RNA SOX21-AS1 sponges miR-145 to promote the tumorigenesis of colorectal cancer by targeting MYO6. Biomed Pharmacother 2017;96:953–959.
46. Mei S, Zong H, Zhou H. Long non-coding RNA PITPNA-AS1 regulates UNC5B expression in papillary thyroid cancer via sponging miR-129-5p. Int J Biol Markers 2021;36:10–19.
47. Ma B, Liao T, Wen D, et al. Long intergenic non-coding RNA 271 is predictive of a poorer prognosis of papillary thyroid cancer. Sci Rep 2016;6:36973.

Received March 23, 2023. Accepted April 24, 2024.

Correspondence:
Address correspondence to: Takahiko Sakaue, MD, PhD, Division of Gastroenterology, Department of Medicine, Kurume University School of Medicine, Kurume, Japan; Liver Cancer Research Division, Research Center for Innovative Cancer Therapy, Kurume University, Kurume, Japan; Division of Gynecologic Oncology, Department of Obstetrics/Gynecology, The Ohio State University Wexner Medical Center, Columbus, Ohio. e-mail: sakaue_takahiko@med.kurume-u.ac.jp.

Acknowledgments:
We thank Yasuko Imamura (Kurume University Research Center for Innovative Cancer Therapy) for technical assistance and Dr Kaori Yasuda (Cell Innovator Co, Ltd) for assisting with microarray data analysis and fruitful discussion. We also thank Editage (www.editage.jp) for the English language editing.

Authors' Contributions:
Takahiko Sakaue, Hironori Koga, and Hideki Iwamoto designed the research. Toru Nakamura, Atsutaka Masuda, Toshimitsu Tanaka, Hiroyuki Suzuki, Hideya Suga, Shingo Hirai, Toru Hisaka, Yoshiki Naito, Keisuke Ohta, and Keiichiro Nakamura participated in data acquisition and interpretation. Takahiko Sakaue wrote the article. Karuppaiyah Selvendiran, Yoshinobu Okabe, Takuji Torimura, and Takumi Kawaguchi supervised the conduct of this study. All authors critically reviewed and revised the manuscript draft and approved the final version for submission.

Conflicts of Interest:
The authors disclose no conflicts.

Funding:
This work was supported by the Private University Research Branding Project of the Ministry of Education, Culture, Sports, Science and Technology (2018–2020), Japan Society for the Promotion of Science (JSPS) KAKENHI Grant Number 19K16844 (2019–2020), The Shin-Nihon Foundation of Advanced Medical Research (2020) and GAP NEXT program (2021).

Ethical Statement:
This study was approved by the Ethical Committee of Kurume University (Kurume, Japan) (Study registration no: 351) and Yanagawa Hospital (Yanagawa, Japan), was conducted according to the Ethical Guidelines for Human Genome/Gene Research enacted by the Japanese Government.

Data Transparency Statement:
All data generated or analyzed during this study are included in this published article and supplementary information files.

Reporting Guidelines:
Helsinki Declaration, STROBE.

Transcript Profiling:
Pancreatic juice-derived microRNA-4516 and microRNA-4674 as novel biomarkers for pancreatic ductal adenocarcinoma: GSE226519, https://www.ncbi.nlm.nih.gov/geo/query/acc.cgi?acc=GSE226519.